All-optical logic based on silicon micro-ring resonators

Qianfan Xu and Michal Lipson

School of Electrical and Computer Engineering, Cornell University
411 Phillips Hall, Ithaca, NY 14853
lipson@ece.cornell.edu

Abstract: We demonstrate all-optical logic in a micron-size silicon ring resonator based on the free-carrier dispersion effect in silicon. We show AND and NAND operation at 310 Mbit/s with ~10-dB extinction ratio. The free-carrier-lifetime-limited bit-rate can be significantly improved by active carrier extraction.

OCIS codes: (130.3120) Integrated optics devices; (200.4660) Optical logic; (250.5300) Photonic integrated circuits

References and Links

1. V. R. Almeida, C. A. Barrios, R. R. Panepucci, and M. Lipson, "All-optical control of light on a silicon chip," Nature **431**, 1081-1084 (2004).
2. Q. Xu, V. R. Almeida, and M. Lipson, "Micrometer-scale all-optical wavelength converter on silicon," Opt. Lett. **30**, 2733-2735 (2005).
3. Q. Xu and M. Lipson, "Carrier-induced optical bistability in silicon ring resonators," Opt. Lett. **31**, 341-343 (2006).
4. T. Tanabe, M. Notomi, S. Mitsugi, A. Shinya, and E. Kuramochi, "Fast bistable all-optical switch and memory on a silicon photonic crystal on-chip," Opt. Lett. **30**, 2575-2577 (2005).
5. T.K. Liang, L.R. Nunes, M. Tsuchiya, K.S. Abedin, T. Miyazaki, D. V. Thourhout, W. Bogaerts, P. Dumon, R. Baets, and H.K. Tsang, "High speed logic gate using two-photon absorption in silicon waveguides," Opt. Commun. **265**, 171-174 (2006).
6. A. Lattes, H. Haus, F. Leonberger, E. Ippen, "An ultrafast all-optical gate," IEEE J. Quantum Electron. **19**, 1718-1723 (1983).
7. T. Fjelde, D. Wolfson, A. Kloch, B. Dagens, A. Coquelin, I. Guillemot, F. Gaborit, F. Poingt, and M. Renaud, "Demonstration of 20 Gbit/s all-optical logic XOR in integrated SOA-based interferometric wavelength converter," Electron. Lett. **36**, 1863-1864, (2000).
8. T. A. Ibrahim, R. Grover, L. C. Kuo, S. Kanakaraju, L. C. Calhoun, and P. T. Ho, "All-optical AND/NAND logic gates using semiconductor microresonators," IEEE Photon. Technol. Lett.**15**, 1422-1424 (2003).
9. T. A. Ibrahim, K. Amarnath, L. C. Kuo, R. Grover, V. Van, and P. T. Ho, "Photonic logic NOR gate based on two symmetric microring resonators," Opt. Lett. **29**, 2779-2781 (2004).
10. B. E. Little, J. T. Laine, and S. T. Chu, "Surface-roughness-induced contradirectional coupling in ring and disk resonators," Opt. Lett. **22**, 4-6 (1997).
11. P. Rabiei, W. H. Steier, C. Zhang, and L. R. Dalton, "Polymer Micro-Ring Filters and Modulators," J. Lightwave Technol. 20, 1968-1975 (2002).
12. R. A. Soref and B. R. Bennett, "Electrooptical effects in silicon," IEEE J. Quantum Electron. **23**, 123-129 (1987).
13. S. F. Preble, Q. Xu, B. Schmidt, and M. Lipson, "Ultra-fast all-optical modulation on a silicon chip," Opt. Lett. **30**, 2891-2893 (2005).

The highly developed micro-fabrication technology enables ultra-compact optical devices integrated on silicon. Recently, all-optical operations, such as all-optical modulation [1,2], optical bistability [3,4], have been demonstrated based on micron-size optical resonators on silicon. The same mechanism can be used to realize all-optical logic functions. Integrated all-optical logic devices have been demonstrated using cm-long silicon [5] or $LiNbO_3$ [6] waveguides, semiconductor optical amplifier based devices [7] or resonators built on III-V

#76244 - $15.00 USD Received 19 October 2006; revised 17 January 2007; accepted 23 January 2007

semiconductors [8,9]. Here, we show the first all-optical logic operation using a compact silicon resonator.

The device used in the experiment consists of a silicon micro-ring resonator coupled to a straight waveguide, as shown in Fig. 1(a). It is fabricated on SOI substrate using E-beam lithography, plasma dry etching, and plasma enhanced chemical vapor deposition (PECVD) for the SiO_2 cladding deposition. The silicon waveguides forming the structure have a width of 450 nm and a height of 250 nm. The radius of the ring is R = 5 μm, and the spacing between the ring and the straight waveguide is 200 nm. The fiber-to-fiber insertion loss for the quasi-TE mode (electric field parallel to the substrate) is measured to be 10.4 dB. The transmission spectrum for the quasi-TE mode is shown in fig. 1(b). One can see from the figure two resonances at the wavelength λ_1 = 1550.7 nm and λ_2 = 1568.7 nm respectively. The transmission of the waveguide drops by about 16 dB at both resonances. The insets of fig. 2 show the zoom-in spectra around both resonant wavelengths. The full-width-half-maximal (FWHM) bandwidths of the resonances are $\Delta\lambda_1$ = 0.14 nm and $\Delta\lambda_2$ = 0.16 nm, corresponding to the quality factors of Q_1 = 11,076 and Q_2 = 9,804, respectively. The power coupling coefficient between the waveguide and the ring can be estimated from the bandwidth to be ~ 7%. The weak split of resonances, represented by the double-notch feature of the resonant spectrum, is caused by a weak reflection inside the ring resonator [10]. The photon lifetime of the ring resonator at λ_1-resonance can be obtained from the quality factor as $\tau_{cav1} = Q \cdot \lambda/(2\pi c)$ = 9.1 ps [11]. This lifetime gives the fundamental limit to the operation speed of the device.

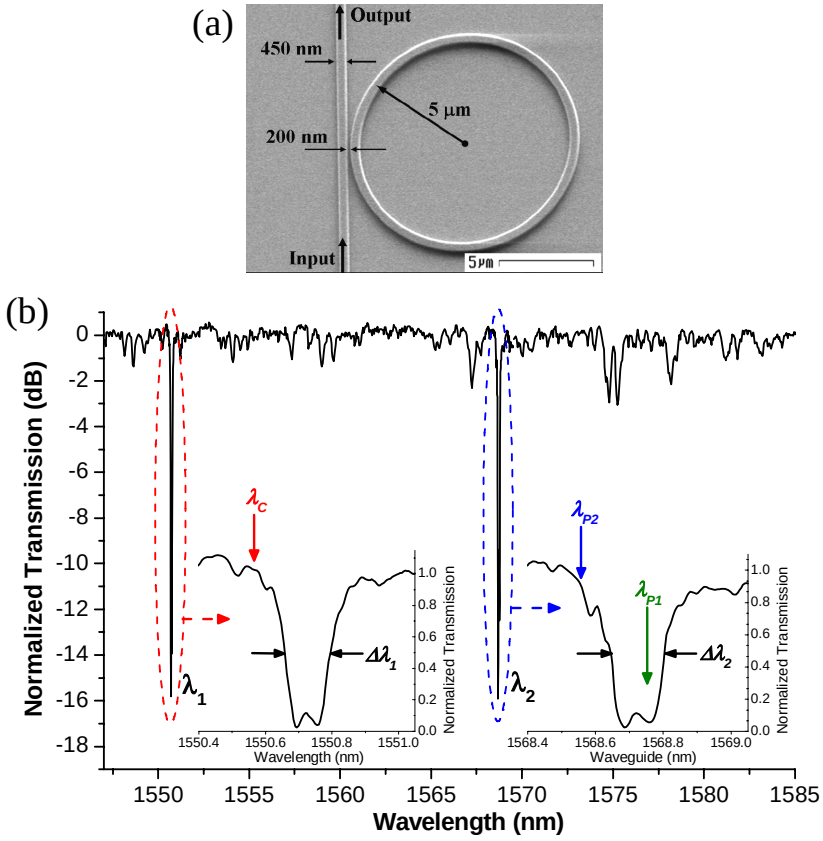

Fig. 1. (a) Top-view SEM picture of the silicon micro-ring resonator before the SiO_2 cladding deposition. (b) The transmission spectrum of the resonator. The insets show the zoom-ins around each resonance. The wavelengths of the pump (λ_C) and the probes for the AND (λ_{P1}) and NAND (λ_{P2}) gates are marked in the insets.

#76244 - $15.00 USD Received 19 October 2006; revised 17 January 2007; accepted 23 January 2007

The logic operation is based on the all-optical modulation mechanism we demonstrated using silicon micro-ring resonators [1]. When a strong optical control pulse and a weak cw probe light are coupled into the ring resonator through two different resonances, the control pulse generates free carriers in the ring resonator due to the two-photon absorption (TPA) effect. The generated free carriers reduce the refractive index of silicon through plasma dispersion effect [12] and blue-shift the ring resonances. The output power of the probe light is modulated by the resonance shift. After the control pulse leaves, the resonant wavelength and the transmission of the probe light relax back due to the fast surface recombination of the free carriers. The relaxation time is determined by the carrier lifetime of ~ 0.5 ns in the ring resonator.

The relationship between the modulation depth and the energy of the control pulse shows a logic-gate-like dependence. In Fig. 2, we show the transfer functions of the all-optical modulation process for both the positive modulation (black line) and the negative modulation (green line) cases, using a 14-ps long Gaussian pulse as the control pulse. A positive modulation is obtained if the wavelength of the probe light is at λ_{P1} in Fig. 1b, so that the device has low transmission without the control pulse, as the black line in the inset of Fig. 2 shows. A negative modulation, shown as the green line in the inset, is obtained at the probe wavelength of λ_{P2} with high transmission before the control pulse comes. Due to the nonlinear nature of the TPA-based process, there is a clear threshold energy of the control pulse to obtain large modulations. One can observe the logic-gate-like behavior on both transfer functions with a sharp transition region sandwiched between flat regions. Specifically, one can see a 10-dB increase of modulation depth on the positive-modulation transfer function when the control pulse energy increases from 2.6 pJ to 5.2 pJ. Similarly, one can see a 10-dB increase of modulation depth on the negative-modulation transfer function when the control pulse energy increases from 4.1 pJ to 8.2 pJ. Therefore, with properly chosen control pulse energy, one can obtain dramatically different modulations with two control pulses together compared to with only one control pulse, enabling logic operations of AND and NAND gates.

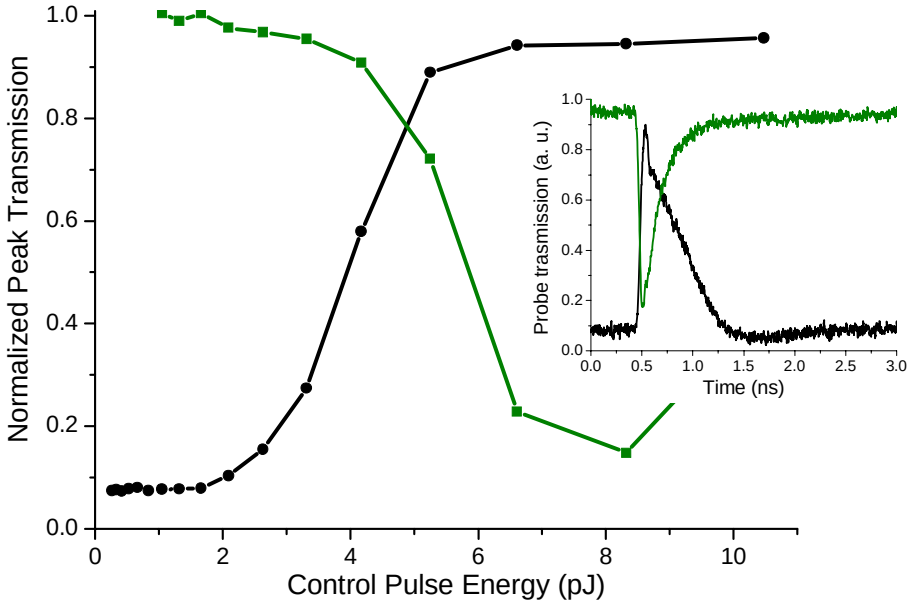

Fig. 2. Transfer function of the all-optical pulse modulation, showing the peak probe transmission immediately after the control pulse versus the control pulse energy inside the silicon waveguide, for the positive modulation (black line) and negative modulation (green line). The inset shows the typical waveform of the probe output for the positive modulation (black line) and negative modulation (green line), respectively.

#76244 - $15.00 USD Received 19 October 2006; revised 17 January 2007; accepted 23 January 2007

The experiment setup used to demonstrate the all-optical logic based on the ring resonator is shown in Fig. 3. A cw light from a tunable laser is modulated with PRBS 2^7-1 return-to-zero (RZ) signal, which is split into two and sent into the device from two opposite directions to avoid the interference between them. The wavelength of the control light is fixed at the shorter-wavelength edge of a resonance of the ring resonator (λ_C), as shown by the blue arrow in Fig. 1b. A cw probe light tuned at another resonance of the ring resonator is coupled together with one of the control signal and sent into the device. The output of the probe light is separated from the control light using an optical circulator and an optical filter. The waveforms of the probe light are then observed on the oscilloscope. The polarization of both control and probe light are set to the TE-like mode by the polarization controllers.

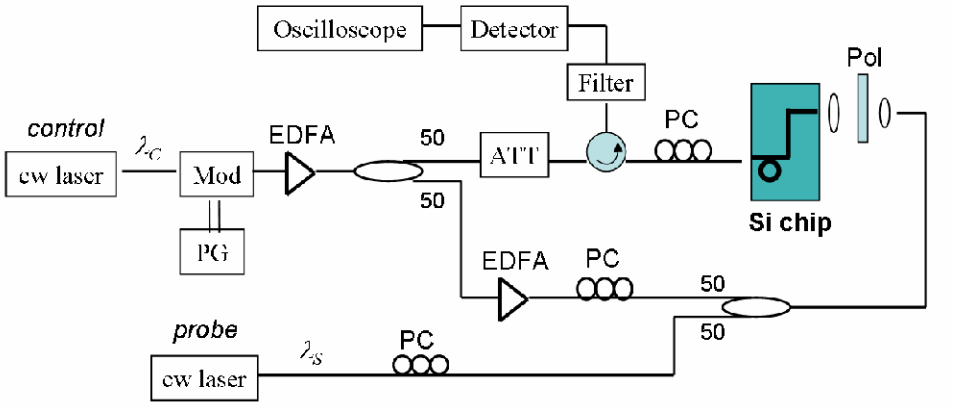

Fig. 3. Schematics of the experiment setup for all-optical logic using silicon ring resonator. PG: pattern generator; Mod: $LiNO_3$ electro-optical modulator; EDFA: erbium-doped fiber amplifier; PC: polarization controller; Pol: polarizer; ATT: attenuator.

The two control signals have bit-rates of 310 Mbit/s and pulse widths of 200 ps. The average optical power inside the silicon waveguide is about 2 mW for each control signal. The pulse energy is therefore about 13 pJ. Note that the switching threshold in this experiment is higher than that shown in Fig. 2, because the wider pulse used here corresponds to a lower peak power and therefore less TPA-based carrier generation for the same pulse energy. The waveforms of these two control signal synchronized at the device are shown in Fig. 4(a) and Fig. 4(b), respectively. When both control signal are in logic '1', which means that the two control pulses are coupled into the ring resonator simultaneously, the total optical power is higher than the threshold to obtain large modulation, and a positive or negative modulation is imposed onto the probe light depending on the wavelength of the probe light. When one or both of the control signals are '0', the total optical power is less than the threshold, and very little modulation is observed on the probe output. This results in the AND ($\lambda_{Probe} = \lambda_{P1}$) and NAND ($\lambda_{Probe} = \lambda_{P2}$) operations with extinction ration ~10 dB, as evident from Fig. 4(c) and Fig. 4(d), respectively. The extinction ratio, which is lower than the 16-dB resonance dip shown in Fig. 1(b), is limited by the small residue modulation associated with the single control pulses as well as by the small misalignment between the probe wavelength and the dip of the resonance. Note that the absorption of the pump pulse generates some heat inside the ring resonator. However, the response time for the thermal effect in the ring resonator is on the order of 1 μs, much longer than the bit-period. Since the temperature only depends on the average power, it is stable in the experiment.

The bit-rate is limited by the free-carrier lifetime in the resonator. In order to avoid inter-symbol interference, a second control pulse has to come in only after all the carriers generated by the first control pulse have recombined. To increase the speed, one can actively extract the carriers from the ring resonator, instead of relying on the recombination of the carriers at the

#76244 - $15.00 USD Received 19 October 2006; revised 17 January 2007; accepted 23 January 2007

Si/SiO_2 interfaces. We have shown that the effective carrier lifetime can be reduced to ~ 30ps by reversely bias a p-i-n junction built across the ring resonator [13], enabling logic operation at ~ 5 Gbit/s.

In conclusion, we have shown experimentally all-optical logic based on silicon micro-ring resonator. Extinction ratio of ~10 dB is achieved with ~2 mW average optical power for each input control signal.

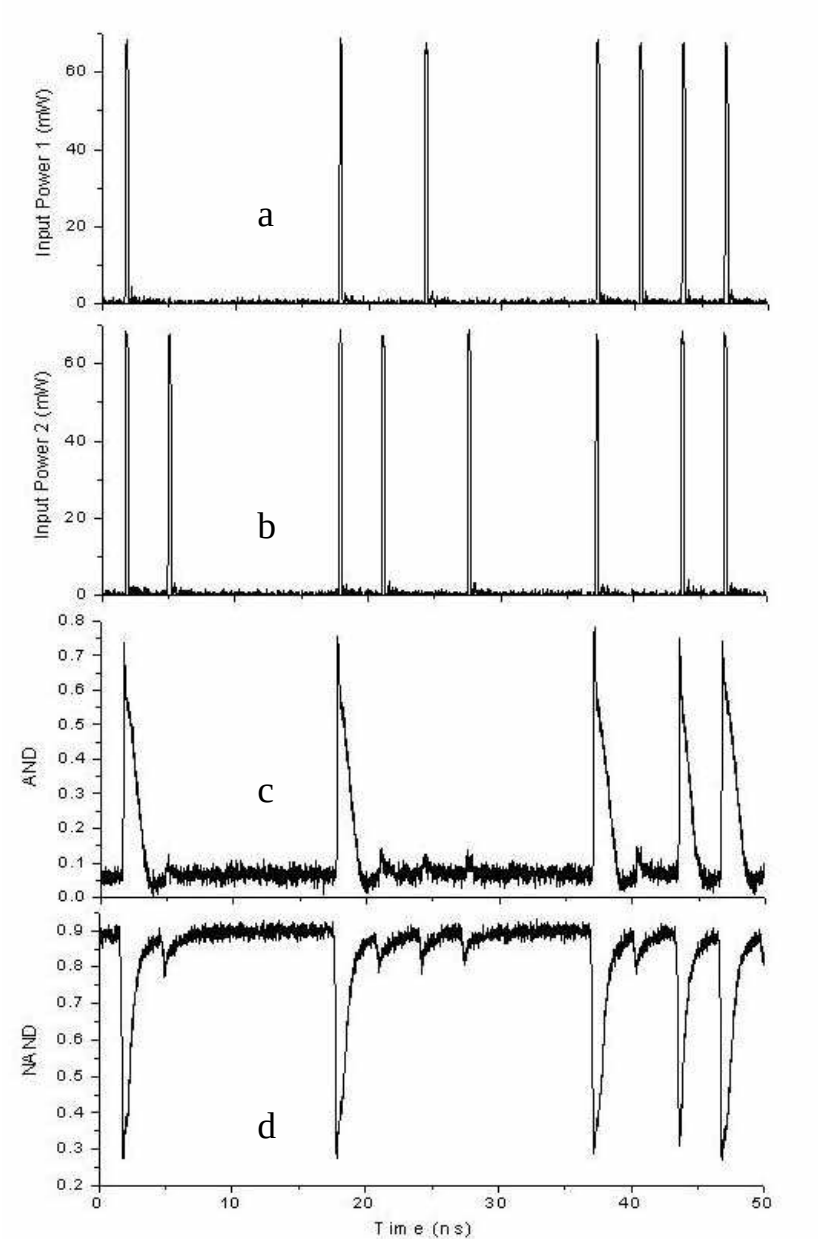

Fig. 4. Waveforms of the control signals and the probe outputs as the logic function of the control signals. (a): waveform of the control input 1. (b): waveform of the control input 2. (c): waveform of the probe light output at $\lambda_{Probe} = \lambda_{P1}$ as the logic AND of the two control inputs. (d): waveform of the probe light output at $\lambda_{Probe} = \lambda_{P2}$ as the logic NAND of the two control inputs.

#76244 - $15.00 USD Received 19 October 2006; revised 17 January 2007; accepted 23 January 2007

Acknowledgments

This work was supported by the Semiconductor Research Corporation under grant number 2005-RJ-1296. The experiments are partially performed at the Cornell Center for Nanoscale Systems, supported by the Nanoscale Science and Engineering Initiative of the National Science Foundation under NSF Award # EEC-0117770 and the New York State Office of Science, Technology & Academic Research under NYSTAR Contract # C020071. The device was fabricated at the Cornell Nano-Scale Science & Technology Facility (CNF), a member of the National Nanotechnology Infrastructure Network (NNIN) which is supported by the NSF, its users, Cornell University and Industrial Affiliates.

#76244 - $15.00 USD Received 19 October 2006; revised 17 January 2007; accepted 23 January 2007